AIAA JOURNAL
Vol. 36, No. 3, March 1998

Predictions of Widespread Fatigue Damage Thresholds in Aging Aircraft

L. Wang*
University of California, Los Angeles, Los Angeles, California 90095
and
W. T. Chow,† H. Kawai,† and S. N. Atluri‡
Georgia Institute of Technology, Atlanta, Georgia 30332-0356

Commercial transport aircraft are required to operate under the concept of damage tolerance. Because of the structural redundancy and the crack arrest capability, the current fleet of commercial aircraft was initially designed to have sufficient residual strength to sustain discrete source damage. However, fatigue damage during the life of an aircraft can significantly reduce the residual strength of an aging aircraft. It is important to predict the threshold for the onset of widespread fatigue damage, i.e., the initiation and growth of cracks at rivet holes (multiple site damage) to threshold sizes at which, in conjunction with a lead crack, the residual strength of the aircraft may fall below the limit load. A hierarchical global–intermediate–local approach is presented for the numerical predictions of the widespread fatigue damage thresholds. A detailed numerical study is presented to illustrate the importance of 1) the use of elastic–plastic fracture mechanics to assess the residual strength and 2) the importance of the local stresses due to rivet misfit, clamping, cold working, fretting, etc., in assessing the number of fatigue cycles to reach the widespread fatigue damage threshold for an aging aircraft.

I. Introduction

THE fatigue damage due to repetitive cabin pressurization is one of the major concerns in the civil aviation industry. There exist two different approaches in dealing with the multiple site fatigue damage problem. One is the multiple site damage threshold (MSDT) approach; the other is the widespread fatigue damage threshold (WFDT) approach.[1] In the MSDT approach the severity of multiple site damage (MSD) is measured by the potential of the site linkup; whereas in the WFDT approach, it is indicated by the reduction of residual strength of the aircraft.

As shown in Fig. 1a, the MSDT approach requires the study of fatigue growth and linkup of a number of small fatigue cracks. If the MSD cracks do not link up between service inspections, it is considered safe. However, small MSD cracks may reduce significantly the residual strength of an aircraft in the presence of a lead crack, as shown in the Fig. 1b. For an aircraft designed to operate at a high level of working stress with a small amount of redundant residual strength, very small undetectable fatigue cracks can reduce the residual strength to below the limit load. On the other hand, an aircraft with sufficient redundant residual strength may be safe in the presence of detectable fatigue cracks. Therefore, using the MSDT approach alone may lead to a false feeling of safety, and the MSDT approach alone is not sufficient for the evaluation of the severity of multiple site fatigue damage on an aircraft.

Currently, the fleet of aging commercial aircraft in the United States is operating under the concept of damage tolerance,[2] which requires that an aircraft have a sufficient residual strength in the presence of damage in the principal structural elements during the interval between service inspections. Such damage includes fatigue cracks, propagating between detectable and critical sizes, and a discrete source damage, induced by foreign objects such as fragments in the case of engine disintegration. Because the fatigue cracks can degrade the damage-tolerance capability of an aircraft, evaluating the severity of fatigue cracks through the evaluation of the reduction in residual strength is very important to truly enforce the damage-tolerance requirement.

From an operational viewpoint, it is important to predict the widespread fatigue damage threshold, i.e., the number of loading cycles that will produce fatigue cracks of such sizes that, in conjunction with a lead crack, will reduce the residual strength of the aircraft to below the limit load. With the knowledge of the widespread fatigue damage threshold, operators of aging aircraft can schedule service inspections economically without compromising safety requirements. This paper presents a hierarchical methodology, based on the finite element alternating method,[3] to predict the WFD threshold, with numerical examples illustrating the typical characteristics of an aging aircraft.

II. Elastic–Plastic Finite Element Alternating Method

Fracture mechanics problems can be solved using a number of different methods, including finite element and boundary element methods, singular/hybrid finite elements, the alternating method, and path-independent and domain-independent integrals, etc.[3–6] As discussed in detail in Ref. 3, the finite element alternating method (FEAM) is considered to be a very efficient and accurate method.[3] The FEAM solves for the cracks (including surface cracks and edge cracks) in finite bodies by iterating between the analytical solution for an embedded crack in an infinite domain and the finite element solution for the uncracked finite body. The cohesive tractions at the locations of the cracks in the finite element (or boundary element) model of the uncracked body and the residuals at the far-field boundaries in the analytical solution for the infinite body are corrected through the iteration process. Essentially, the alternating method is a linear superposition method.

Fracture mechanics parameters can be found accurately, because the near crack tip fields are captured exactly by the analytical solution. Coarser meshes can be used in the finite element analysis because the cracks are not modeled explicitly. In a crack growth analysis, or in conducting a parametric analysis with various crack sizes, the stiffness of the uncracked body remains the same for all crack sizes. Thus, the global stiffness matrix of the finite element model is decomposed only once. In the most common finite element analysis for fracture problems, it is necessary to use very fine meshes (or adaptive mesh refinements) around the crack tips and to decompose the global stiffness matrix every time a crack size changes. Thus, the alternating method is very efficient in saving

Received March 10, 1997; revision received Nov. 20, 1997; accepted for publication Nov. 20, 1997.

*Postdoctoral Fellow, Center for Aerospace Research and Education.
†Postdoctoral Fellow, Computational Modeling Center.
‡Institute Professor, Regents' Professor of Engineering, Hightower Chair in Engineering, and Director, Computational Modeling Center. Fellow AIAA.

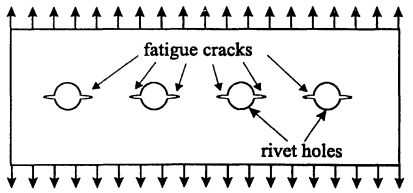

When will these fatigue cracks link up ?

a) MSD threshold

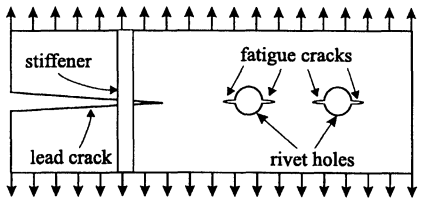

When will the panel lose the capability to stop the lead crack ?

b) WFD threshold

Fig. 1 MSD and WFD threshold approaches.

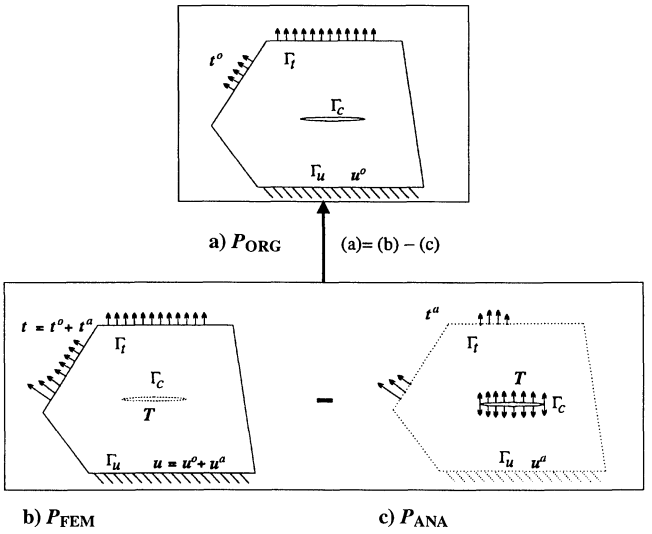

Fig. 2 Superposition principle for FEAM.

both time in the computational analysis and human effort in the mesh generation.[3]

Early applications of the Schwartz–Neumann alternating method in fracture mechanics involved solving edge crack problems in plane strain[7] and surface circular/elliptical cracks in three-dimensional bodies.[8–11] However, the earlier alternating method[10] for the analysis of surface flaws was not able to give accurate results because of the lack of a general analytical solution in an infinite body for an embedded crack subjected to arbitrary crack face tractions. The continuous effort of Atluri and his colleagues (see Refs. 12–19) in developing and exploring the general analytical solutions for embedded cracks in an infinite body, subjected to arbitrary crack surface loads, makes the FEAM both efficient and accurate.

The FEAM can be applied to an elastic–plastic analysis of cracks when it is used in conjunction with the initial stress method, even though the alternating method itself is based on the linear superposition principle. The initial stress approach converts the elastic–plastic analysis into a series of linear elastic steps, in each of which the superposition principle holds. The elastic–plastic finite element method was first presented in Nikishkov and Atluri.[20] It was used in two-dimensional elastic–plastic analyses of widespread fatigue damage in ductile panels.[21] The elastic–plastic finite element alternating method (EPFEAM) was used in simulating stable crack growth in the presence of MSD, using the T^* integral criterion,[3,4] in a series of recent reports.[22–24] In these reports, the stable tearing test data on 10 wide flat panels, conducted at the National Institute of Standards and Technology, was simulated using EPFEAM. The numerical predictions of the load vs crack growth curve for each of these 10 test specimens were within 15% of the test data, even for the panels with 10 MSD cracks ahead of each lead crack tip. Encouraged by this success of the numerical methodology, it is being applied to study the WFDT in curved, stiffened fuselage panels in the present paper.

A. Schwartz–Neumann Alternating Method

The alternating method uses the following two simpler problems to solve the problem of a cracked finite size body. The first one, denoted P_{ANA}, is shown in Fig. 2c. (Figure 2 shows only one crack. Many cracks may be present.) The first problem is that of the same cracks in an infinite domain subjected to the unknown crack surface loading $\boldsymbol{T}$. The second one, denoted P_{FEM} (Fig. 2b), has the same finite geometry as in the original problem except that the cracks are ignored. The boundary Γ_u of P_{FEM} has the prescribed displacement $\boldsymbol{u}$, whereas the boundary Γ_t has the prescribed traction $\boldsymbol{t}$. The prescribed displacements and tractions are different from those in the original problem in general. Because of the absence of the cracks, the problem P_{FEM} can be solved much easier by the finite element method. The alternating procedure for solving the cracked body is outlined as follows.

1) Solve P_{FEM} with the given load on the boundary Γ. Solve for the tractions, which are used to close the cracks. Denote the solution as S_1^{FEM}, where 1 indicates that this is the solution for the first iteration,

$$S_1^{FEM} : \boldsymbol{T}^{(1)} = \boldsymbol{K}^u \boldsymbol{u}^0 + \boldsymbol{K}^t \boldsymbol{t}^0$$

2) Reverse the crack surface traction obtained in the preceding step and apply it as the load on the crack surfaces and solve the P_{ANA}. Denote the solution S_1^{ANA},

$$-S_1^{ANA} : \begin{Bmatrix} \boldsymbol{u} \\ \boldsymbol{t} \end{Bmatrix}^{(1)} = \begin{Bmatrix} \overline{\boldsymbol{K}^u} \\ \overline{\boldsymbol{K}^t} \end{Bmatrix} \boldsymbol{T}^{(1)}$$

3) Find the tractions on the boundary Γ_t and the displacements on the boundary Γ_u from the analytical solutions obtained in the preceding step. Reverse them as the load for P_{FEM}. Find the crack-closing tractions from the solution S_2^{FEM},

$$S_2^{FEM} : \boldsymbol{T}^{(2)} = \boldsymbol{K}^u \boldsymbol{u}^{(1)} + \boldsymbol{K}^t \boldsymbol{t}^{(1)}$$

4) Repeat steps 2 and 3 until the residual load is small enough to be ignored:

$$-S_i^{ANA} : \begin{Bmatrix} \boldsymbol{u} \\ \boldsymbol{t} \end{Bmatrix}^{(i)} = \begin{Bmatrix} \overline{\boldsymbol{K}^u} \\ \overline{\boldsymbol{K}^t} \end{Bmatrix} \boldsymbol{T}^{(i)}$$

$$S_{i+1}^{FEM} : \boldsymbol{T}^{(i+1)} = \boldsymbol{K}^u \boldsymbol{u}^{(i)} + \boldsymbol{K}^t \boldsymbol{t}^{(i)}$$

for $i = 2, 3, \ldots$.

The solution to the original problem is the summation of all those obtained in the alternating procedure, i.e.,

$$S = \sum_{i=1}^{n} \left(S_i^{FEM} + S_i^{ANA} \right) \tag{1}$$

B. Analytical Solutions for a Single Crack Subjected to Piecewise Linear Crack Surface Tractions

Explicit solutions for an infinite body containing a single crack, the faces of which are subjected to point loads, and piecewise constant/linear loads can be obtained.[3,6] Using these localized forms of loading on the crack surfaces, one can construct solutions for complicated crack surface tractions by superposition, as opposed to starting out constructing solutions for smooth and continuously distributed crack face tractions, such as polynomial variations. Point loading gives the simplest solution. But point loading causes an artificial redistribution of crack surface tractions. This leads to poor stress solutions at the crack surface. The generic solution for a point loading can be used in the linear elastic analysis, where the stress

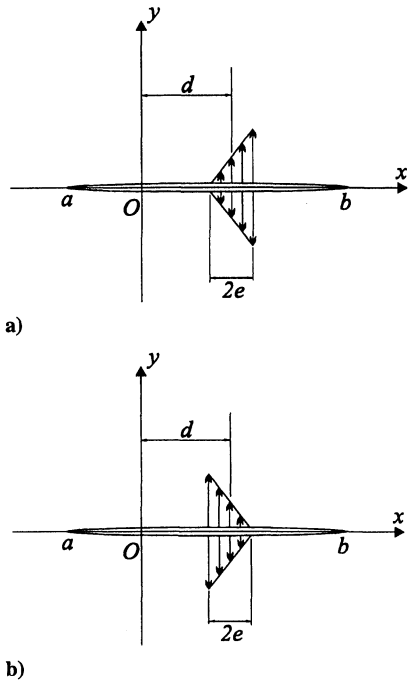

Fig. 3 Crack in an infinite domain, subjected to piecewise linear crack surface tractions.

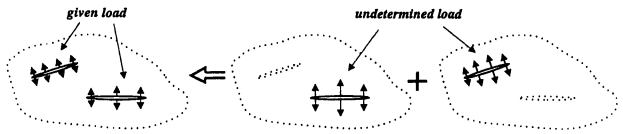

Fig. 4 Superposition of the single-crack solutions to find the multiple-crack solution.

solution around the crack surface is not an important solution goal, as long as the stress intensity factor, which is of primary interest, can be obtained directly. However, piecewise constant/linear crack face loads should be used as the generic solutions, to construct a solution for an arbitrary crack face loading in an elastoplastic analysis, because capturing the stress state near the crack is essential to compute the elastic–plastic fracture parameters.

It is assumed that the crack (Fig. 3) $\overline{ab}$ is on the real axis. The x coordinates of the left and the right crack tips of the crack are a and b. The complete analytical solution for the problem shown in Fig. 3 is documented in Refs. 3 and 6 and is not repeated here.

C. Solutions for Multiple Embedded Cracks

Solutions for multiple embedded cracks in an infinite body, subjected to arbitrary crack surface tractions, can be constructed using the solution for a single crack in an infinite body subjected to arbitrary crack surface loading. Analytical solutions for multiple embedded cracks in an infinite body are available only for some special configurations, such as multiple collinear cracks subjected to arbitrary crack surface tractions.[25] There are several implementations of the FEAM based on such analytical solutions.[18,19] It is, in general, easier to construct the solution of multiple embedded cracks in an infinite body using the solution for a single embedded crack. Solutions for arbitrary distributions of cracks can be obtained using this approach. It can be more accurate and efficient to build the multiple crack solutions from that for a single crack even when the analytical solution is available, such as for the multiple collinear cracks in an infinite domain.

Consider the superposition of n solutions of single cracks in the infinite body. Each of these n solutions involves only one crack. Denote the k'th solution as S_k, where the crack is at the same location as that of the k'th crack of the original multiple-crack problem. The crack surface traction $\boldsymbol{T}_k$ for the problem S_k ($k = 1, 2, \ldots, n$) is to be determined (Fig. 4).

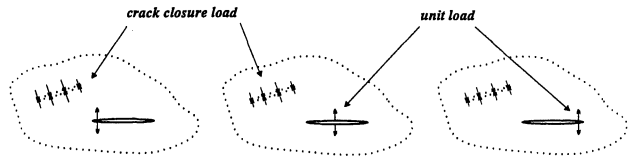

Fig. 5 Evaluation of the tractions at the locations of cracks for each load in terms of unit basis functions.

The traction at the location of the jth crack in the problem S_k can be found for any load $\boldsymbol{T}_k$, i.e.,

$$\boldsymbol{t}_{jk} = \boldsymbol{K}_j^{[k]}\boldsymbol{T}_k, \qquad j, k = 1, 2, \ldots, n \tag{2}$$

It is noticed that $\boldsymbol{K}_k^{[k]} = \boldsymbol{I}$ ($k = 1, 2, \ldots, n$) are identity operators because the tractions at the crack surfaces are the same as the applied loads.

The superposition of the n solutions should give back the original problem, i.e., the tractions at the locations of the crack surfaces should be the same as the given crack surface loads. Thus, the linear system to be solved is

$$\sum_{k=1}^{n} \boldsymbol{t}_{jk} = \sum_{k=1}^{n} \boldsymbol{K}_j^{[k]}\boldsymbol{T}_k = \boldsymbol{T}_j^0, \qquad j = 1, 2, \ldots, n \tag{3}$$

We can denote collectively the undetermined crack surface loads, $\boldsymbol{T}_k$ ($k = 1, 2, \ldots, n$), as $\boldsymbol{T}$. Similarly, denote collectively the given loads, $\boldsymbol{T}_k^0$ ($k = 1, 2, \ldots, n$), as $\boldsymbol{T}^0$. Thus, Eq. (3) can be rewritten as

$$\boldsymbol{K}\boldsymbol{T} = \boldsymbol{T}^0 \tag{4}$$

where $\boldsymbol{K}$ is a linear operator. Once the linear operator $\boldsymbol{K}$ is evaluated numerically, we can solve the linear system for the unknown traction $\boldsymbol{T}$.

The procedure to solve the multiple-crack problem is outlined as follows.

1) Apply loads in terms of unit basis functions on one of the cracks, ignoring the other cracks. Use the analytical solution for a single crack to solve the tractions at the locations of all of the other cracks (Fig. 5).

2) Approximate these tractions in terms of the linear combination of the basis functions. Find the magnitude of each component.

3) Approximate the given crack surface load $\boldsymbol{T}_k$ in terms of the linear combination of the basis functions. Find the magnitude of each component.

4) Solve the linear system Eq. (4) to obtain the loads applied on each single-crack solution.

5) Superimpose the n single-crack solutions to form a solution for the original problem.

The coefficients of the linear system remain the same in the analysis of the same cracks under different loadings, because they depend only on the crack configuration and the basis functions. Thus, the linear system can be solved for different loads without recomputing the coefficients of the system. This feature is particularly useful when the constructed multiple-crack solution is used in the FEAM, where it is necessary to evaluate the solution for the same cracks under different loadings during the alternating procedure.

D. Elastoplastic Analysis of Multiple Cracks in a Finite Body

Elastoplastic analysis can be carried out by the initial stress method,[26] which reduces the nonlinear analysis to a series of linear analyses, for which the principle of superposition holds. Thus, the FEAM can be used to perform these linear analyses.

The initial stress method can be described as the following. Assuming no body forces, the virtual work principle is

$$\int_{\Omega} \boldsymbol{\sigma} : \delta\nabla\boldsymbol{u}\, \mathrm{d}\Omega = \int_{\Gamma_t} \boldsymbol{t}^0 \cdot \delta\boldsymbol{u}\, \mathrm{d}\Gamma \tag{5}$$

where $\boldsymbol{\sigma}$ is the elastoplastic stress, $\boldsymbol{t}^0$ is the prescribed surface traction, Ω is the domain of the body, and Γ_t is the boundary with prescribed tractions.

First, the elastic prediction is found by assuming that the deformation is entirely elastic. The elastoplastic stress $\boldsymbol{\sigma}^p$ within the body

is found by using the displacements obtained in the linear elastic analysis. But σ^p may not satisfy the equilibrium equations. Let σ^c be the undetermined correction for the stress, i.e., $\sigma = \sigma^p + \sigma^c$. Substituting this into Eq. (5), we find that σ^c satisfies

$$\int_\Omega \sigma^c : \delta\nabla u \, d\Omega = \int_{\Gamma_t} t^0 \cdot \delta u \, d\Gamma - \int_\Omega \sigma^p : \delta\nabla u \, d\Omega \qquad (6)$$

The right-hand side of the equation can be viewed as the virtual work done by the unbalanced force. The left-hand side of Eq. (6) is the virtual work done by the correction stress. The elastic estimate of the correction stress σ^c can be solved by the alternating method for the linear elastic analysis. The new elastic prediction for the displacements is the sum of the old one and the correction term. This correction procedure is repeated until the unbalanced force becomes negligible.

The elastoplastic analysis of the cracked structures using the initial stress method and the FEAM can be outlined as follows.

1) Solve the crack closure traction using the finite element method, assuming that the material is elastic. Denote the solution of displacement gradients as $F^{\text{FEM}}_{(1)}$:

$$T^{(1)} = K^u u^0 + K^t t^0$$

$$F^{\text{FEM}}_{(1)} = F^u u^0 + F^t t^0$$

where K^u and K^t and F^u and F^t are linear operators. $T^{(1)}$ is the traction used to close the crack.

2) Reverse the traction obtained in step 1 and apply it as the load on the crack surfaces. Denote the analytical solution of displacement gradient $F^{\text{ANA}}_{(1)}$

$$F^{\text{ANA}}_{(1)} = -F^T T^{(1)}$$

where F^T is a linear operator.

3) Compute the elastoplastic stress due to the displacement gradient $F^{\text{FEM}}_{(1)} + F^{\text{ANA}}_{(1)}$:

$$\sigma^p_{(1)} = R\left(F^{\text{FEM}}_{(1)} + F^{\text{ANA}}_{(1)}\right)$$

where R is a nonlinear operator.

4) Compute the boundary load $u^{(1)}$ and $t^{(1)}$ and the distributed load $f^{(1)}$ due to the incorrectness of the stress $\sigma^p_{(1)}$.

5) Apply the loads $u^{(1)}$, $t^{(1)}$, and $f^{(1)}$ on the uncracked body, assuming that the material is elastic. Repeat the procedure of finding residuals until the process converges:

$$T^{(i+1)} = K^u u^{(i)} + K^t t^{(i)} + K^f f^{(i)}$$

$$F^{\text{FEM}}_{(i+1)} = F^u u^{(i)} + F^t t^{(i)} + F^f f^{(i)}$$

$$F^{\text{ANA}}_{(i+1)} = F^T T^{(i+1)}$$

$$\sigma^p_{(i+1)} = R\left(\sum_{j=1}^{i+1} \left(F^{\text{FEM}}_{(j)} + F^{\text{ANA}}_{(j)}\right)\right)$$

for $i = 1, 2, \ldots$, where K^f and F^t are also linear operators.

This procedure can be applied using the deformation theory of plasticity, which is valid for a cracked structure undergoing monotonic proportional loading. For a plastic material undergoing loading/unloading, it is only valid for the first loading step using a J_2 flow theory of plasticity, i.e., loading the unstressed body to the given level of boundary load. But similar procedures can be applied to any loading/unloading precess: the deformation gradient in the procedure should be replaced by its increment for the loading step. The stress is determined from the previous stress state and the increment of displacement gradient. In the analysis of crack growth, the newly created crack surfaces, in general, experience plastic deformation. To remove the crack closure stress, a step of evaluating elastoplastic stress at the crack surface must be added before the evaluation of the analytical solution for cracks in the infinite domain.

III. Effects of MSD Cracks on Residual Strength

To determine the critical MSD crack size that will reduce the residual strength of an aircraft fuselage to below the limit load, one must perform a residual strength analysis of the fuselage in the presence of a lead crack and MSD. Nonlinear material behavior must be considered in such a study. At the critical load, the plastic zone size ahead of the lead-crack tip in a typical cracked aircraft fuselage is as large as half an inch to several inches. However, the typical rivet spacing is only about 1 in. Therefore, the zone of plastic deformation ahead of the lead crack is not negligible when compared to the size of the MSD cracks and the uncracked ligaments ahead of the lead crack. In an elastic fracture mechanics model, the deformation and stress are highly localized near the crack tip. Because of the plastic deformation, these stresses must be redistributed along the ligaments to achieve static equilibrium, as suggested in Irwin's model for the estimation of plastic zone size. Such a stress redistribution can significantly change the loading condition of the adjacent cracks in the MSD crack situation. On the other hand, the existence of MSD cracks limits the size of the ligaments on which the stress can be redistributed. Furthermore, the stress redistribution is much more complicated in the MSD situation due to the interaction between the MSD cracks and the lead crack. Therefore, a detailed elastic–plastic fracture analysis of the cracked panel is necessary.

Figure 6a shows a typical MSD situation in a flat panel, in which there is a single lead crack located at the center of the flat panel. There are two small cracks ahead of each of the lead-crack tips. The length of the ligaments between adjacent cracks is 1 in. The material is assumed to be AL 2024-T3. A piecewise linear flow curve is used for AL 2024-T3, as shown in Fig. 6b. When only the lead crack is considered to be present, the applied far-field tension for which the crack tip K factor, as calculated from linear elastic fracture mechanics (LEFM), reaches the critical value K_{IC} is designated as σ^f_{LE}. The normalized residual strength, shown in Fig. 7, is the ratio $(\sigma^f - \sigma^A)/(\sigma^f_{\text{LE}} - \sigma^A)$, where σ^f is the failure stress in the different cases shown in Fig. 7 and σ^A is the applied far-field stress. Thus,

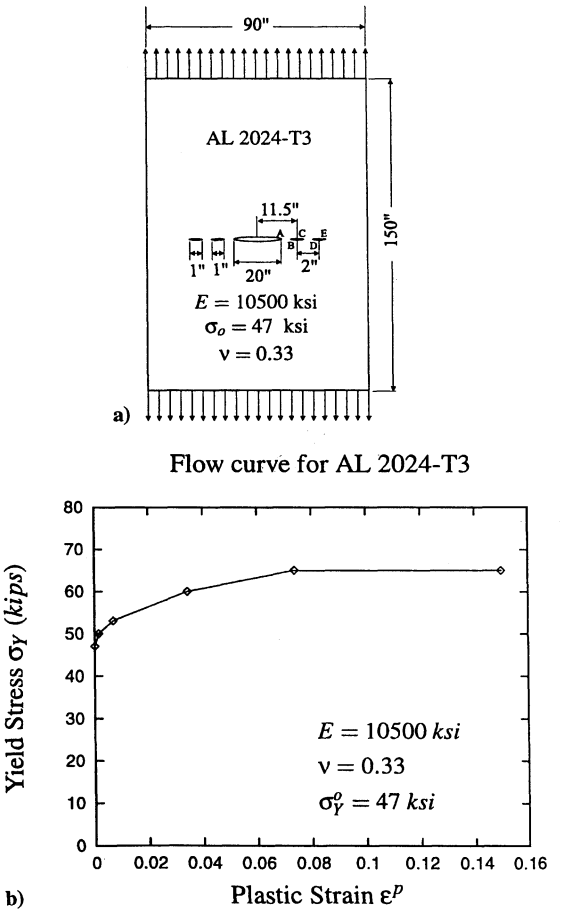

Fig. 6 Lead crack and MSD in a flat sheet.

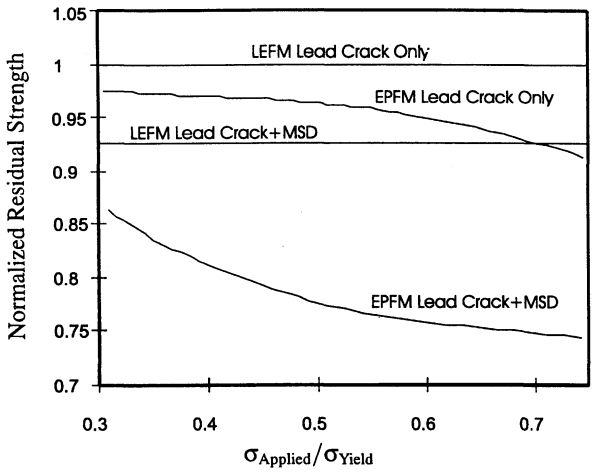

Fig. 7 Normalized residual strength for 1) the lead crack only, using LEFM; 2) the lead crack only, using EPFM; 3) the lead crack with MSD, using LEFM; and 4) the lead crack with MSD, using EPFM.

when LEFM is used, with only a lead crack, the normalized residual strength is 1, irrespective of the applied stress. In the case of a lead crack plus MSD, when LEFM is used, the K factor at the lead crack tip reaches K_{IC} sooner; the failure stress is, thus, lower than when only the lead crack is present and, thus, the normalized residual strength in the case is lower, as shown in Fig. 7. On the other hand, when elastic–plastic fracture mechanics (EPFM) is used, when only a lead crack is present, the normalized residual strength depends on σ^A and is always lower than in the case when LEFM is used. In the EPFM case, σ^f is defined as the stress at which the value of the J integral reaches the critical value of J_{IC} at the lead crack-tip. Finally, when EPFM is used and when the case of a lead crack plus MSD is considered, the residual strength is much lower than in the other three cases and depends on σ^A. Thus, it is clear from Fig. 7 that LEFM overestimates the residual strength as compared to the EPFM approach. Thus, in the presence of MSD cracks, the LEFM approach can lead to significant error, especially if the panel is operating at a high-stress level. This illustrative example, as well as the analytical–experimental comparisons for flat panels that are already well documented in Refs. 22–24 form the motivation in using EPFM to analyze the WFD threshold in curved, stiffened fuselage panels in the present paper.

IV. Residual Strength Analyses of Aircraft Fuselages

The global–intermediate–local hierarchical modeling is an efficient approach for the residual strength analyses of aircraft fuselages, in the presence of a lead crack and MSD. Figure 8 graphically shows such a hierarchical approach. In a global analysis, linear elastic analyses of global load flow in the aircraft fuselage are carried out using the ordinary finite element method. Stringers and frames are simplified as straight beams and curved beams. Skins are modeled using shell elements. Lead cracks are modeled explicitly. However, no mesh refinement around crack tips is necessary because the purpose of the analysis is to obtain the load flow pattern, i.e., to obtain the boundary conditions for the detailed intermediate model.

The intermediate model contains a smaller portion of the cracked fuselage, where stringers and frames are modeled in detail, using shell elements. Each rivet is modeled individually using spring elements. The empirical formula suggested by Swift[27] is used to model the flexibility of rivets. Thus, the influence of the detailed structure on the membrane stress in the skin can be determined through this linear elastic intermediate analysis. Again, the lead crack is modeled explicitly, but no mesh refinement around the crack tip is made to reduce the computational cost.

A rectangular skin model is obtained from the intermediate analysis. In the local model the boundary loading conditions at the four edges and the rivet pin loads on the rivet holes are obtained from the intermediate analysis. The skin-only local model is analyzed using the elastic–plastic alternating method, where none of the cracks is modeled explicitly. Analytical solutions for an embedded crack in

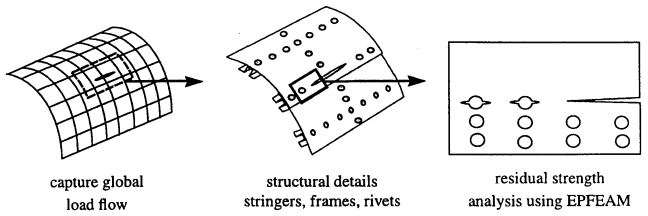

Fig. 8 Global–intermediate–local hierarchical approach for the residual strength analysis of an aircraft fuselage.

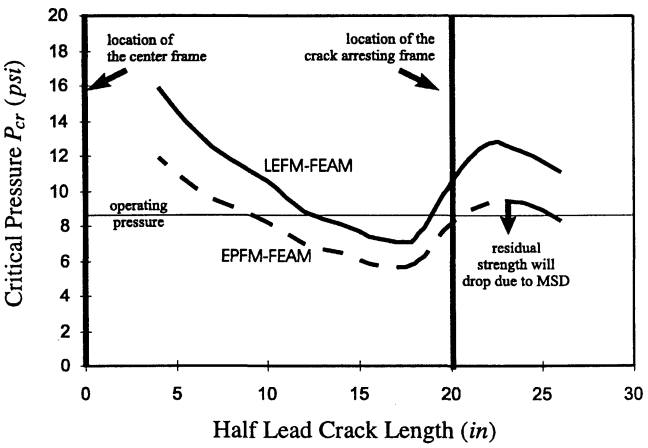

Fig. 9 Residual strength curve for the lead crack only case.

an infinite domain, subjected to arbitrary crack surface loadings, are used to capture the singular fields near the crack tips.

A typical residual strength plot obtained from such a global–intermediate–local analysis is shown in Fig. 9. In the analysis shown in Fig. 9, we assume that the aircraft fuselage has a radius of 118 in. The longitudinal lead crack is located at a lap joint splice. We assume a broken center tear strap while the center frame remains intact. The skin thickness is 0.071 in. The critical stress intensity factor for the skin is taken as $K_{Ic} = 90\ \text{ksi}\sqrt{\text{in}}$. Rivets are of radius 0.095 in. The frame spacing is 20 in. The stringer spacing is 10 in.

Figure 9 shows the critical cabin pressure P_{cr} vs the half-crack length a of the lead crack. The critical pressure is defined as the cabin pressure at which the stress intensity factor (or its equivalent elastic–plastic counterpart, T^*, which is same as J for stationary cracks) at the lead-crack tip reaches the critical value. It is seen that the residual strength (in this case, simply the critical cabin pressure) reaches a local maximum shortly after the lead crack penetrates the first crack arresting frame. In the numerical modeling, we assume that the crack arresting frame remains intact and the tear strap under the crack arresting frame is broken when the lead crack penetrates the crack arresting frame. The residual strength curve is obtained by computing the critical pressure for different sizes of the lead crack. Therefore, no stable tearing is considered. It is seen that the linear elastic analysis significantly overestimates the residual strength of the cracked fuselage.

The local maximum (Fig. 9) is above the operating pressure, which is assumed to be 8.4 psi. Therefore, if a large damage, due to a linkup of the fatigue cracks and/or a foreign impact, is induced during the operation, the lead crack will be arrested around the local maximum at the operating pressure, provided that the damage extends to no more than two bays. However, MSD cracks ahead of the lead crack can bring down the local maximum to below the operating pressure. In such a case, the fuselage no longer has the required crack arresting capability. The aircraft with MSD can still operate with sufficient strength, provided no large damage is present in the fuselage. However, it becomes vulnerable to damage, because it no longer has the capability to arrest a two-bay damage.

Figure 10 shows how the residual strength (based on EPFM) at the local maximum point (see Fig. 9; at this point, half the lead-crack length is about 22.5 in.) decreases as the number and the sizes of fatigue cracks ahead of the lead-crack tip increase. Here, we assume equal length fatigue cracks to be emanating from both sides of a rivet

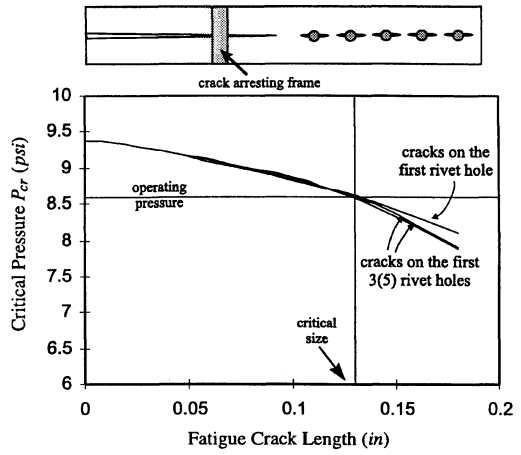

Fig. 10 Residual strength in the presence of MSD cracks.

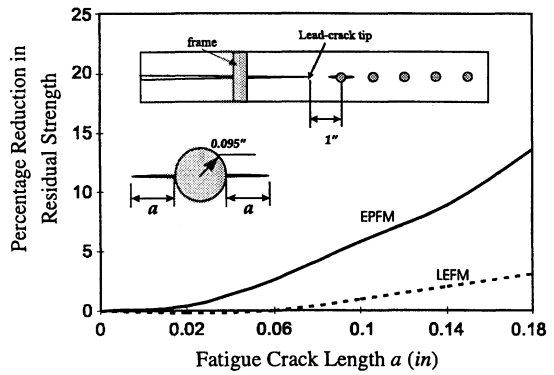

Fig. 11 Reduction in residual strength for the case of fatigue cracks emanating from the first rivet hole ahead of the lead-crack tip.

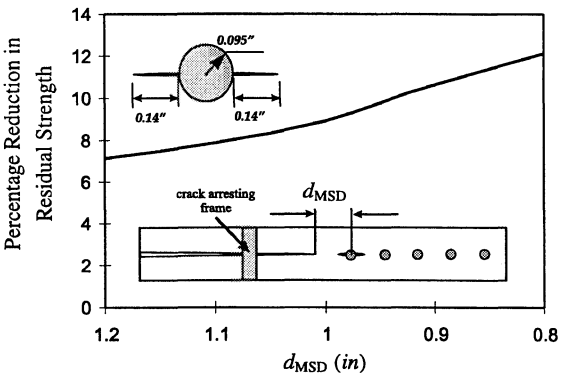

Fig. 12 Influence of d_{MSD}, the distance between the lead-crack tip and center of the first rivet hole, on the reduction in residual strength.

hole. The crack lengths are measured from the edges of rivet holes to the tips of fatigue cracks. The distance between the lead-crack tip and the center of the first rivet hole is 1 in. Three different MSD cases are presented. They correspond to fatigue cracks emanating from 1) the first rivet hole ahead of the lead-crack tip, 2) the first three rivet holes ahead of the lead-crack tip, and 3) the first five rivet holes ahead of the lead-crack tip. From this analysis, we can find the critical sizes of fatigue cracks that will pose a widespread fatigue damage (WFD) problem.

Figure 11 shows the reduction of residual strength for the MSD case in which there are only two equal-length fatigue cracks emanating from the first rivet hole ahead of the lead-crack tip, as indicated in the figure. The result obtained using the LEFM approach and the result obtained using the EPFM approach are shown in Fig. 11. It is seen that LEFM predicts a very small reduction in residual strength. Thus, using LEFM will lead to a false impression that this structure is too strong to have WFD problems. Therefore, we conclude that EPFM approach is mandatory in the study of WFD problem.

The reduction of residual strength also depends strongly on d_{MSD}, the distance between the lead-crack tip and center of the first rivet hole. The smaller d_{MSD} is, the stronger the influence of MSD cracks. Figure 12 shows such an effect. From another point of view, the discrete source damage is random in nature. A probabilistic description seems to be more natural, and a probabilistic analysis is more suitable than a deterministic analysis.

V. Fatigue Crack Growth Analyses

After the analyses of the effect of MSD on the crack arresting capability of the aircraft fuselage panel, one can perform fatigue crack growth analyses to determine the threshold number of fatigue cycles corresponding to the WFD threshold. Such an analysis is illustrated in the following. The hierarchical modeling strategy described in the preceding section is also used for the fatigue analysis. The local fatigue analysis uses FEAM and LEFM. Figure 13 shows the results from a simple, straightforward fatigue analysis. The Forman et al.[28] crack growth equation is used in the analysis. It is

$$\frac{da}{dN} = \frac{C(\Delta K)^n}{(1-R)K_c - \Delta K} \tag{7}$$

where ΔK is the stress intensity factor range and R is the stress ratio in cyclic loading. [In the example (without considering the effect of residual stress), $K_{min} = 0$ and $R = 0$.] The values of K_c, C, and n were given by Forman et al.[28] as the following:

$$K_c = 83\,\text{ksi}\sqrt{\text{in.}}$$

$$C = 3 \times 10^{-4}\,\text{kcyc}\,\text{ksi}^{-2}\,\text{in.}^{-2}$$

$$n = 3$$

These correspond to the material AL 2024T3. In this example, the initial rivet-hole-crack size of 0.02 in. is considered, as this represents a typical size for a nondetectable crack under the rivet head. A numerical–experimental comparison reported in a separate study on a full-scale test panel[29] and the excellent correlation reported in Ref. 3 using the same analytical approach as the present lend credence to the results in Fig. 13.

However, the residual stress near rivet holes can change the fatigue life of these MSD cracks significantly. Residual stress due to misfitting, cold working, rivet clamping forces, fretting, etc., can all change the fatigue behavior. The simplified model proposed by Park and Atluri[18] to account for residual stress due to interference fit and cold working is used in this paper to demonstrate the effect of residual stresses on the fatigue analyses. The simplified model is described as follows.

In this simplified model,[18] rivets are assumed to be rigid. This assumption is made so as to allow use of an elastic–plastic analytical solution[18] for the shrink-fit problem of an oversized rivet into the rivet hole, as will be briefly described. The effective amount of misfitting, which accounts for the expansion of the rivet hole, is used to compute the residual stress due to the misfitting and the corresponding stress intensity factors, as explained briefly subsequently.

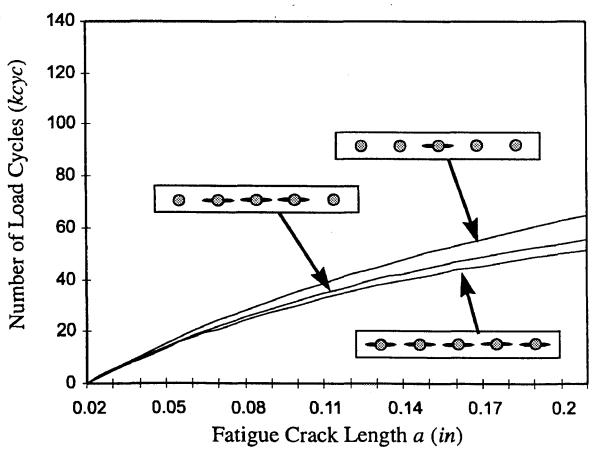

Fig. 13 Fatigue crack growth without considering the effect of residual stress.

Consider a rivet with interference fit. The rivet has a radius that is larger than that of the hole by an amount v_0. The residual stress due to the interference fit is considered to be equivalent to a constant residual radial pressure on the hole surfaces. The likely partial separation between the rivet and the hole surface is not considered. Neither is the effect of friction.

For a single hole with a radius R in an infinite sheet, with a rivet of radius $(R + v_0)$ being inserted into the hole, the relation between the radial pressure on the hole surface and its radial displacement v_0 is[25]

$$p_0 = (2\mu)(v_0/R) = k_0(v_0/R) \tag{8}$$

For convenience, we denote k_0 as the stiffness of the hole in an infinite sheet for purposes of the initial stresses. Equation (8) is for a perfect hole without cracks.

In the presence of fatigue cracks emanating from the hole, the stiffness of the hole, k_a, will be a function of the crack length. The local residual stress due to the misfitting of amount v_0 is

$$p_a = k_a(v_0/R) \tag{9}$$

or

$$k_a = v_0 p_a/R \tag{10}$$

The FEAM can be used to solve for the stress intensity factor.

It is assumed that the rivet misfit is equal to v_0 for all of the fastener holes in a row and that the initial radial pressure on each hole in a row of fastener holes, without cracks and any far-field loading, is equal in magnitude to p_0 as in Eq. (8).

When the radial displacement v at the hole surface, due to the far-field loads only, i.e., without considering the misfitting, is greater than v_0, there is no longer a misfit between the hole and the rivet. When it is smaller than v_0, the effective amount of misfitting is $v_0 - v$. The radial pressure exerted due to misfitting is

$$p_a = \begin{cases} k_a(v_0 - v)/R & \text{when } v < v_0 \\ 0 & \text{when } v \geq v_0 \end{cases} \tag{11}$$

Therefore, the stress intensity factors due to the rivet misfitting for the crack emanating from the hole, subjected to the far-field load, can be obtained.

The cold working generally induces a plastic deformation near the hole. The plastic residual stress near the hole, due to the cold working, is determined first from a simple one-dimensional axial symmetric analysis. The effect of this residual stress field on the crack tip stress intensity factor is then determined. It is assumed that the plastic deformation is caused solely by cold working of the fastener hole and that the applied far-field hoop stress does not produce any plastic deformation. The material is regarded to be elastic-perfectly-plastic.

When the radial pressure p_0 applied on the hole surface is small, the material deforms elastically, and the stress field near the hole can be expressed as

$$\sigma_{rr} = -p_0(R/r)^2 \tag{12}$$

$$\sigma_{\theta\theta} = p_0(R/r)^2 \tag{13}$$

where r is the distance from the center of a hole of radius R.

As the pressure p_0 increases, the material near the hole begins to deform plastically. Let the region $R \leq r \leq r_y$ deform plastically, and the region outside this deforms elastically. The stress field can be obtained by solving the corresponding field equations, with the simple Tresca yield condition. The stresses in the plastically deformed region are

$$\sigma_{rr} = -p_0 + \sigma_{ys}\, \ln(r/R), \qquad R \leq r \leq r_y \tag{14}$$

$$\sigma_{\theta\theta} = (\sigma_{ys} - p_0) + \sigma_{ys}\, \ln(r/R), \qquad R \leq r \leq r_y \tag{15}$$

The stresses in the elastic region are

$$\sigma_{rr} = -(\sigma_{ys}/2)(r_y/r)^2, \qquad r > r_y \tag{16}$$

$$\sigma_{\theta\theta} = (\sigma_{ys}/2)(r_y/r)^2, \qquad r > r_y \tag{17}$$

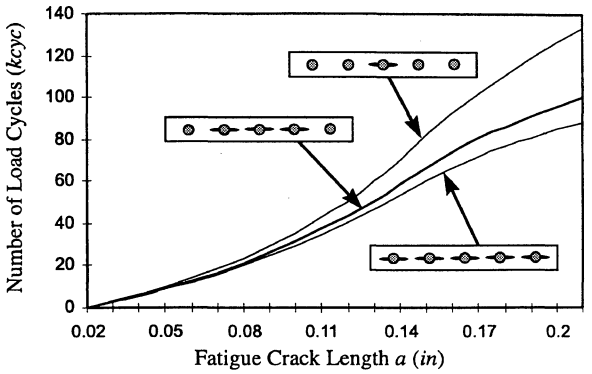

Fig. 14 Fatigue crack growth considering the effect of residual stress.

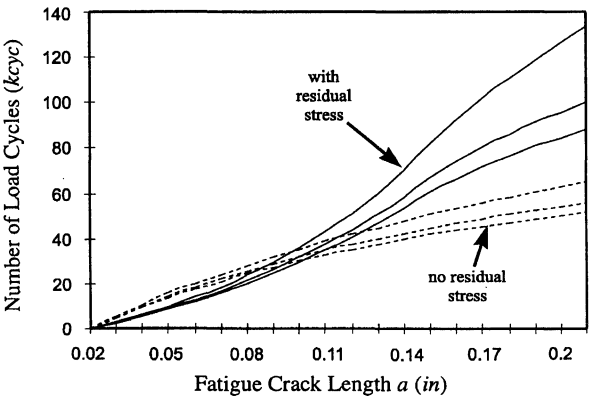

Fig. 15 Fatigue crack growth with and without considering the effect of residual stresses.

where σ_{ys} is the yield strength of the material and r_y is the radius of the plastic region. They are related to p_0 as

$$p_0 = \sigma_{ys}\left[\tfrac{1}{2} + \ln(r_y/R)\right] \tag{18}$$

Figure 14 shows the prediction of fatigue growth with the consideration of residual stress, assuming that the rivet misfitting induces an initial residual stress that is three times the far-field stress. In the results shown in Fig. 14, the stress ratio R was increased to $0.03 \sim 0.05$ due to the residual stress near the rivet hole. It is seen that in the presence of residual stress the fatigue growth behavior changes significantly. When compared to the case where there is no residual stress, as seen in Fig. 15, the small cracks grow faster and large cracks grow slower. Thus, the catch-up phenomenon due to such residual stress, i.e., small fatigue cracks may grow faster to catch up with the sizes of large cracks, may be observed. Park and Atluri[18] presented details with more examples on the catch-up phenomenon.

However, this analysis is based on a simplified residual stress model. In practice, misfitting and cold working are displacement-controlled processes. A more elaborate procedure may be needed to evaluate the effect of misfitting, clamping, and cold working. Again, due to the random nature of the residual stresses a probabilistic analysis is necessary.

Considering the results from the residual strength analyses (see Fig. 10) and the results from the fatigue analyses (Fig. 15), one can determine the fatigue damage threshold, i.e., the critical fatigue crack size that will reduce the residual strength of the structure to below the limit load and the number of pressurization cycles that will lead to fatigue damages of that size.

VI. Conclusions

It is necessary to use the WFDT approach to study the effect of MSD on the crack arresting capability of an aircraft fuselage to truly enforce the damage tolerance requirement. With the knowledge of WFDT, operators of aging aircraft can schedule service inspections economically without compromising safety requirements, and

the aircraft designer can optimize aircraft designs for better trade-off between production cost, operating cost, maintenance cost, and structural strength redundancy. Plasticity is very important in the residual strength analysis of not only the lead crack in the presence of MSD, but also of the lead crack itself. Residual stresses, induced by rivet misfitting, cold working, rivet clamping forces, fretting, etc., can change significantly the fatigue crack growth in an aircraft fuselage and thus profoundly affect the number of fatigue cycles corresponding to the WFD threshold. Detailed studies to estimate more accurately the effects of the various residual stress are needed, especially the effect of partial contact between the hole and the rivet, the effect of friction, and the effect of rivet clamping force. Because discrete source damages are random events and the magnitude of residual stresses has a large scatter, a probabilistic analysis as a follow-up of the present deterministic analysis is necessary.

Acknowledgments

The authors would like to acknowledge the support from the office of the Dean of the School of Engineering and Applied Sciences at the University of California, Los Angeles, to the first author, and from the FAA Center of Excellence at Georgia Institute of Technology.

References

[1]Jeong, D. Y., and Tong, P., "Threshold of Multiple Site Damage in Aging Airplanes," *Structural Integrity in Aging Aircraft*, ASME-AD Vol. 47, American Society of Mechanical Engineers, New York, 1995, pp. 63–71.

[2]Swift, T., "The Influence of Slow Stable Growth and Net Section Yielding on the Residual Strength of Stiffened Structure," *13th International Committee on Aeronautical Fatigue* (Pisa, Italy), May 1985.

[3]Atluri, S. N., *Structural Integrity and Durability*, Tech Science Press, Forsyth, GA, 1997.

[4]Atluri, S. N., *Computational Methods in the Mechanics of Fracture*, North-Holland, Amsterdam (also in Russian, Mir Publishers, Moscow), 1986.

[5]Atluri, S. N., and Nishioka, T., "On Some Recent Advances in Computational Methods in the Mechanics of Fracture," *Advances in Fracture Research*, Plenary Lecture, Proceedings of the 7th International Conference on Fracture (ICF7), Vol. 3, 1989, pp. 1923–1969.

[6]Wang, L., and Atluri, S. N., "Recent Advances in the Alternating Method for Elastic and Inelastic Fracture Analyses," *Computer Methods in Applied Mechanics and Engineering*, Vol. 137, No. 1, 1996, pp. 1–58.

[7]Lachenbruch, A. H., "Depth and Spacing of Tension Cracks," *Journal of Geophysical Research*, Vol. 66, No. 12, 1961, pp. 4273–4292.

[8]Smith, F. W., Emery, A. F., and Kobayashi, A. S., "Stress Intensity Factors for Semicircular Cracks: Part 2—Semi-Infinite Solid," *Journal of Applied Mechanics*, Vol. 34, No. 4, 1967, pp. 953–959.

[9]Thresher, R. W., and Smith, F. W., "Stress-Intensity Factors for a Surface Crack in a Finite Solid," *Journal of Applied Mechanics*, Vol. 39, No. 1, 1972, pp. 195–200.

[10]Shah, R. C., and Kobayashi, A. S., "Stress Intensity Factors for an Elliptical Crack Approaching the Surface of a Semi-Infinite Solid," *International Journal of Fracture*, Vol. 9, No. 2, 1973, pp. 133–146.

[11]Sih, G. C., *Mechanics of Fracture 1: Methods of Analysis and Solutions of Crack Problems*, Noordhoff International, Leyden, The Netherlands, 1973.

[12]Vijayakumar, K., and Atluri, S. N., "An Embedded Elliptical Crack, in an Infinite Solid, Subjected to Arbitrary Crack-Face Tractions," *Journal of Applied Mechanics*, Vol. 103, No. 1, 1981, pp. 88–96.

[13]Nishioka, T., and Atluri, S. N., "Analytical Solution for Embedded Elliptical Cracks, and Finite Element Alternating Method for Elliptical Surface Cracks, Subjected to Arbitrary Loadings," *Engineering Fracture Mechanics*, Vol. 17, No. 3, 1983, pp. 247–268.

[14]O'Donoghue, P. E., Nishioka, T., and Atluri, S. N., "Multiple Surface Cracks in Pressure Vessels," *Engineering Fracture Mechanics*, Vol. 20, No. 3, 1984, pp. 545–560.

[15]Simon, H. L., O'Donoghue, P. E., and Atluri, S. N., "Finite-Element-Alternating Technique for Evaluating Mixed Mode Stress Intensity Factors for Part-Elliptical Surface Flaws," *International Journal for Numerical Methods in Engineering*, Vol. 24, No. 4, 1987, pp. 689–709.

[16]Liao, C. Y., and Atluri, S. N., "Stress Intensity Factor Variation Along a Semicircular Surface Flaw in a Finite-Thickness Plate," *Engineering Fracture Mechanics*, Vol. 34, No. 4, 1989, pp. 957–976.

[17]Rajiyah, H., and Atluri, S. N., "Analysis of Embedded and Surface Elliptical Flaws in Transversely Isotropic Bodies by the Finite Element Alternating Method," *Journal of Applied Mechanics*, Vol. 113, No. 2, 1991, pp. 435–443.

[18]Park, J. H., and Atluri, S. N., "Fatigue Growth of Multiple-Cracks Near a Row of Fastener-Holes in a Fuselage Lap-Joint," *Computational Mechanics*, Vol. 13, No. 3, 1993, pp. 189–203.

[19]Wang, L., and Atluri, S. N., "Implementation of the Schwartz–Neumann Alternating Method for Collinear Multiple Cracks with Mixed Type of Boundary Conditions," *Computational Mechanics*, Vol. 16, No. 4, 1995, pp. 266–271.

[20]Nikishkov, G. P., and Atluri, S. N., "Analytical-Numerical Alternating Method for Elastic-Plastic Analysis of Cracks," *Computational Mechanics*, Vol. 13, No. 6, 1994, pp. 427–442.

[21]Pyo, C. R., Okada, H., and Atluri, S. N., "Residual Strength Prediction for Aircraft Panels with Multiple Site Damage, Using the EPFEAM for Stable Crack Growth Analysis," *Computational Mechanics*, Vol. 16, No. 3, 1995, pp. 190–196.

[22]Wang, L., Brust, F. W., and Atluri, S. N., "The Elastic-Plastic Finite Element Alternating Method and the Prediction of Fracture Under WFD Conditions in Aircraft Structures," *Computational Mechanics*, Vol. 19, No. 5, 1997, pp. 356–369.

[23]Wang, L., Brust, F. W., and Atluri, S. N., "The Elastic-Plastic Finite Element Alternating Method (EPFEAM) and the Prediction of Fracture Under WFD Conditions in Aircraft Structures. Part II. Fracture and the T^*-Integral Parameter," *Computational Mechanics*, Vol. 19, No. 5, 1997, pp. 370–379.

[24]Wang, L., Brust, F. W., and Atluri, S. N., "The Elastic-Plastic Finite Element Alternating Method (EPFEAM) and the Prediction of Fracture Under WFD Conditions in Aircraft Structures. Part III. Computational Predictions of the NIST Multiple Site Damage Experimental Results," *Computational Mechanics*, Vol. 20, No. 3, 1997, pp. 199–212.

[25]Muskhelishvili, N. I., *Some Basic Problems of the Mathematical Theory of Elasticity*, Noordhoff, Groningen, The Netherlands, 1953.

[26]Nayak, G. C., and Zienkiewicz, O. C., "Elasto-Plastic Stress Analysis: A Generalization for Various Constitutive Relations Including Strain Softening," *International Journal of Numerical Methods in Engineering*, Vol. 5, 1972, pp. 113–135.

[27]Swift, T., "Fracture Analysis of Stiffened Structures," *Damage Tolerance of Metallic Structures*, ASTM STP 842, American Society for Testing and Materials, 1984, pp. 69–107.

[28]Forman, R. G., Kearney, V. E., and Engle, R. M., "Numerical Analysis of Crack Propagation in Cyclic-Loaded Structures," *Journal of Basic Engineering*, Vol. 89, 1967, pp. 459–464.

[29]Samavedam, G., Hoadley, D., and Thomson, D., *Full Scale Testing and Analysis of Fuselage Panels*, Foster–Miller, Waltham, MA, 1992.

R. K. Kapania
Associate Editor